Supplemental Figure 1

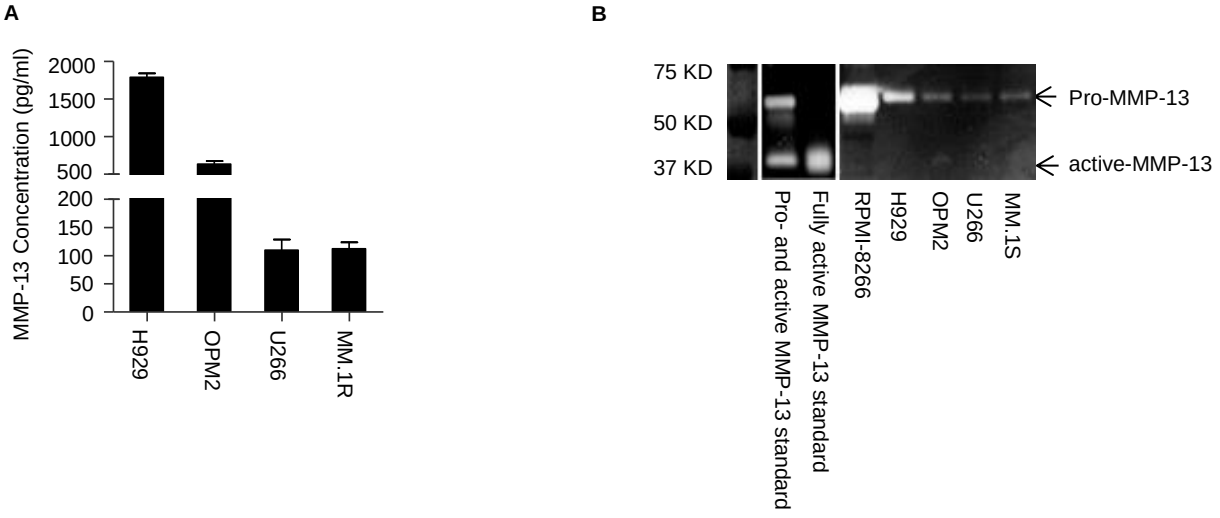

Supplemental Figure 1. MMP-13 expression in MM cells. (A) Supernatants from human MM cells lines were collected after a 72 h incubation period and MMP-13 total protein levels were determined by MMP-13 fluorimetric assay (mean ± SD; n=3). The data are representative of 2 independent experiments. **(B)** Supernatants from human MM cells lines were concentrated and MMP-13 processing determined by collagen zymography. A mixture of pro-MMP-13 (MW: 60 KD) and active MMP-13 (MW: 48 KD) or fully active MMP-13 protein (MW: 48 KD) standards were loaded as controls. White dividing lines indicate the rearrangement of the standard samples from a parallel gel. The data are representative of 3 independent experiments.

Supplemental Figure 2

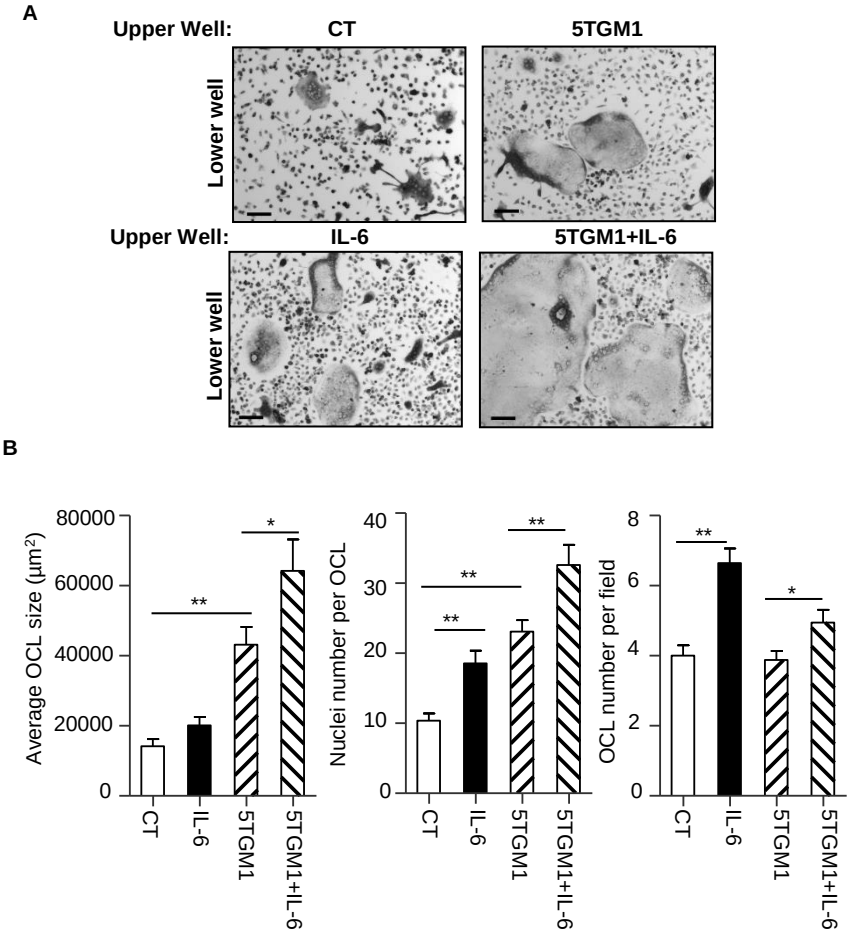

Supplemental Figure 2. IL-6 increases MM-induced OCL fusion. Mouse non-adherent bone marrow cells were co-cultured with or without 5TGM1 cells in Transwell dishes in the presence of M-CSF (10 ng/ml) and RANKL (50 ng/ml) for 4 d to induce OCL differentiation. IL-6 (20 ng/ml) was added as indicated. **(A)** OCLs were stained for TRAP and images captured as described in *Methods*. Scale bar, 100 μm. (**B)** OCL size (left panel), nuclei number per OCL (middle panel) and OCL number per field (right panel) were determined microscopically with ImageJ software (mean ± SEM; n=3). **P* ≤ 0.05, ***P* ≤ 0.01 by ANOVA (left panel) or Poisson ANOVA (middle and right panels).

Supplemental Figure 3

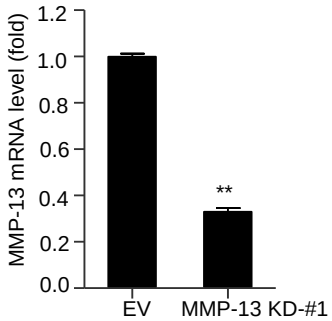

Supplemental Figure 3. MMP-13 expression in mouse 5TGM1-GFP MM cell lines. MMP-13 mRNA levels were determined in 5TGM1-GFP-EV and 5TGM1-GFP-MMP-13 KD-#1 cells by quantitative RT-PCR (mean ± SD; n=3). ***P* ≤ 0.01 by Student's *t*-test. The data are representative of 6 independent experiments.

Supplemental Figure 4

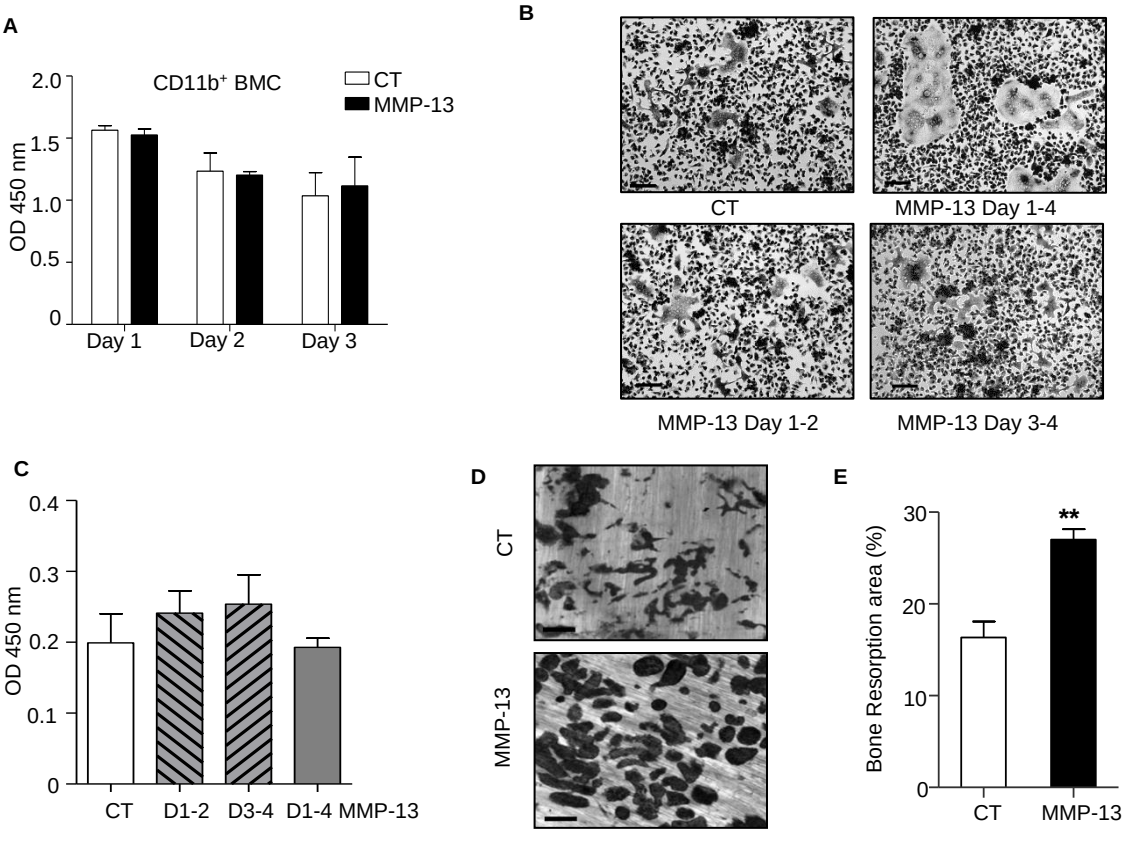

Supplemental Figure 4. MMP-13 enhances OCL bone resorption activity. (A) 1×10^5 mouse CD11b$^+$ bone marrow cells were cultured in 96 well plates with M-CSF (100 ng/ml) and RANKL (50 ng/ml) with or without MMP-13 (200 ng/ml) for up to 3 d. Cell proliferation was determined by WST-1 assay. The data are representative of 3 independent experiments. **(B-C)** 1×10^5 mouse CD11b$^+$ bone marrow cells were cultured in 96 well plates with M-CSF (100 ng/ml) and RANKL (50 ng/ml) for 4 days. MMP-13 (200 ng/ml) were added in the culture during day 1-2, day 3-4 or day 1-4 as indicated. On day 4, OCLs were stained by TRAP (B); cell proliferation was determined by WST-1 assay (C). Scale bar, 100 μm. **(D-E)** Human non-adherent bone marrow cells were seeded atop dentin slices and cultured with or without pro-MMP-13 during OCL formation in the presence of M-CSF (10 ng/ml) and RANKL (50 ng/ml) for 21 d. Bone resorption lacunae were stained with hematoxylin and visualized by microscopy. Scale bar, 100 μm (D). Bone resorption area was calculated by ImageJ software (mean ± SEM; n=3) (E). $^{**}P \leq 0.01$ by Student's *t*-test. The data are representative of 3 independent experiments.

Supplemental Figure 5

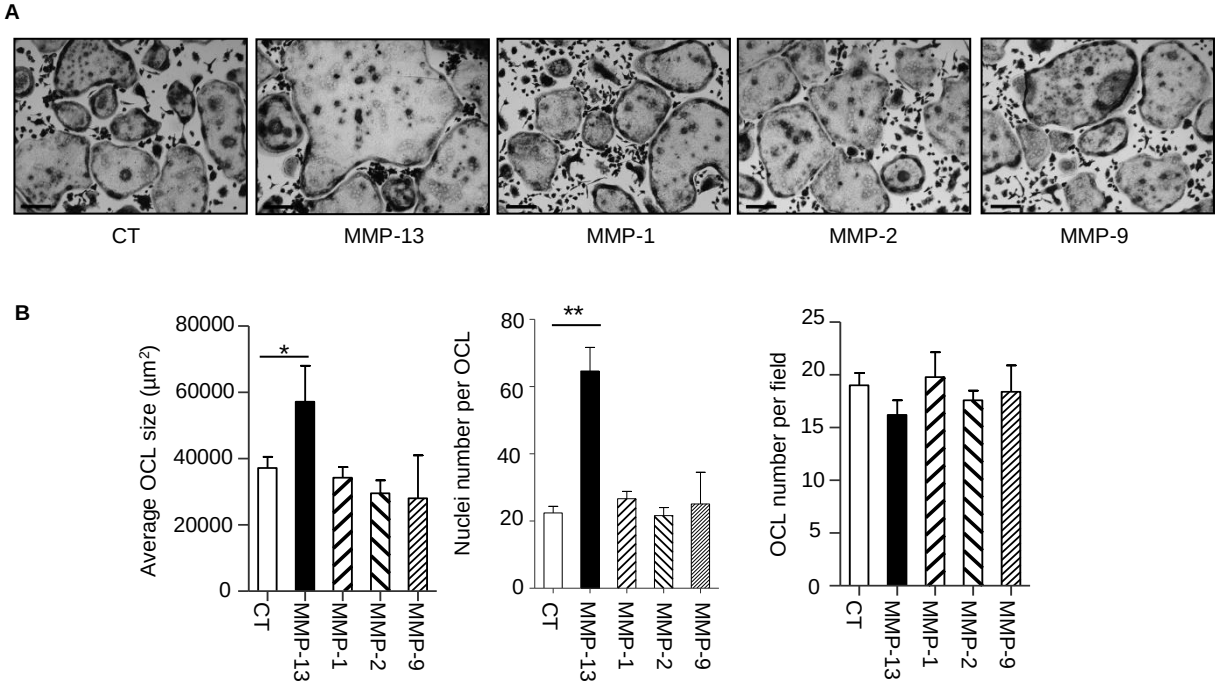

Supplemental Figure 5. MMP-1, 2 and 9 fail to induce OCL fusion. (A) Mouse non-adherent bone marrow cells were cultured with or without 200 ng/ml pro-MMP-13, pro-MMP-1, pro-MMP-2, pro-MMP-9 or vehicle during OCL formation for 4 d. OCLs were stained for TRAP and images captured as described in *Methods*. Scale bar, 100 µm. The data are representative of 3 independent experiments. The data are representative of 4 independent experiments. **(B)** Mouse OCL size (left panel), nuclei number per OCL (middle panel) and OCL number per field (right panel) were determined microscopically using ImageJ software (mean ± SEM; n=3). *$P \leq 0.05$, **$P \leq 0.01$ by ANOVA (left panel) or Poisson ANOVA (middle and right panels).

Supplemental Figure 6

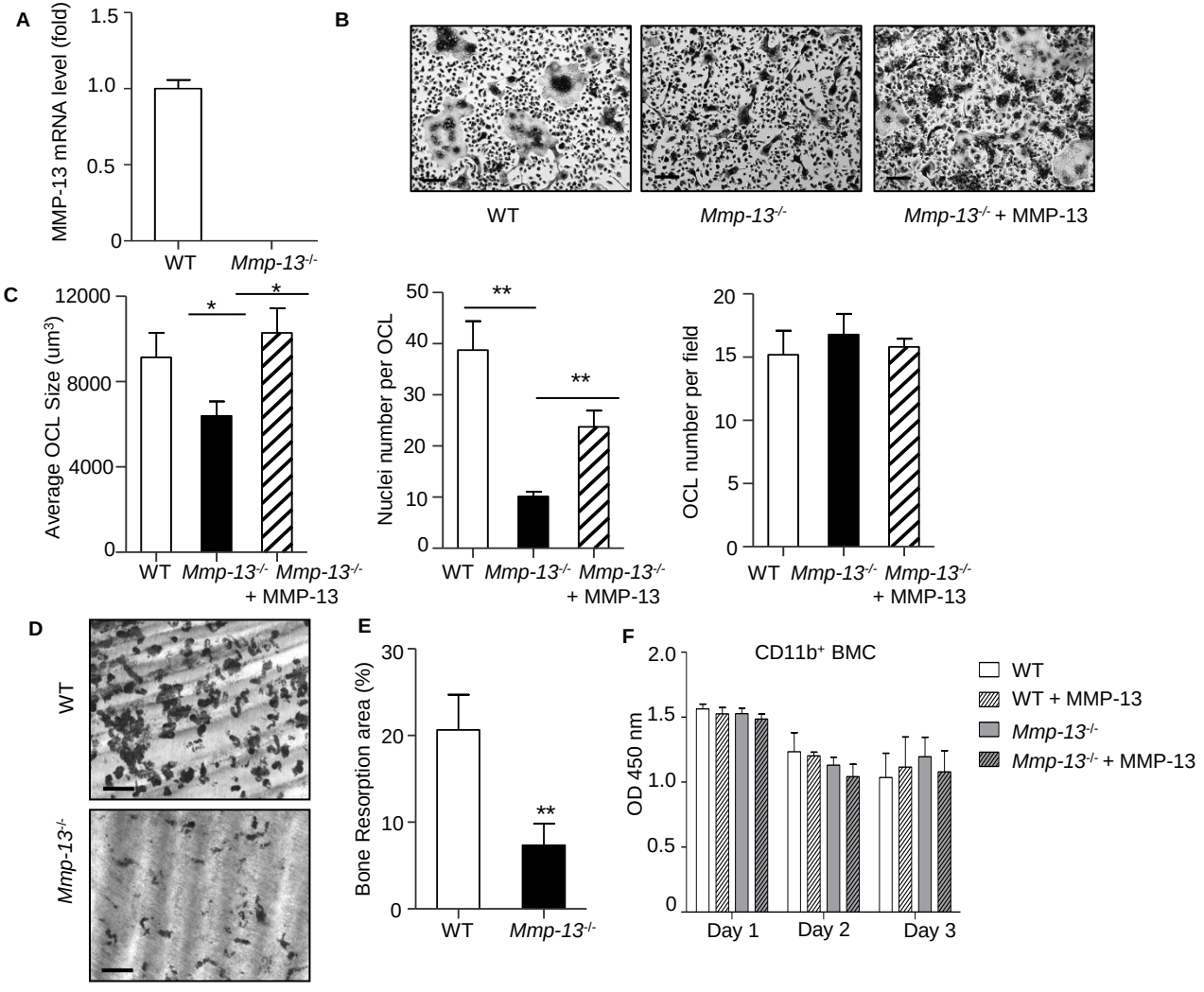

Supplemental Figure 6. Impaired OCL formation and bone resorption activity in *Mmp-13*$^{-/-}$ MNCs. WT or *Mmp-13*$^{-/-}$ mouse non-adherent bone marrow cells were cultured in the presence of M-CSF (10 ng/ml) and RANKL (50 ng/ml) for 4 d to induce OCL formation. **(A)** MMP-13 mRNA levels were determined by quantitative RT-PCR (mean ± SD; n=3). **(B)** For rescue experiments, pro-MMP-13 (200 ng/ml) was added to *Mmp-13*$^{-/-}$ mononuclear cells. OCLs were stained for TRAP and images captured as described in *Methods*. Scale bar, 100 μm. **(C)** OCL size (left panel), nuclei number per OCL (middle panel) and OCL number per well (right panel) were determined microscopically using ImageJ software (mean ± SEM; n=3). **P* ≤ 0.05, ***P* ≤ 0.01 by ANOVA (left panel) or Poisson ANOVA (middle and right panels). The data are representative of 3 independent experiments. **(D)** Non-adherent bone marrow cells were isolated from WT or *Mmp-13*$^{-/-}$ mice and seeded atop dentin slices treated as described in (B) for 9 d. Bone resorption lacunae were stained with hematoxylin and the images captured by light microscopy. Scale bar, 100 μm. **(E)** Bone resorption area was calculated using ImageJ software (mean ± SEM; n=3). ***P* ≤ 0.01 by Student's *t*-test. **(F)** 1×10^5 CD11b$^+$ cells from WT and *Mmp-13*$^{-/-}$ mice were cultured to induce OCL differentiation with or without MMP-13. Cell proliferation was determined by WST-1 assay. The data are representative of 2 independent experiments.

Supplemental Figure 7

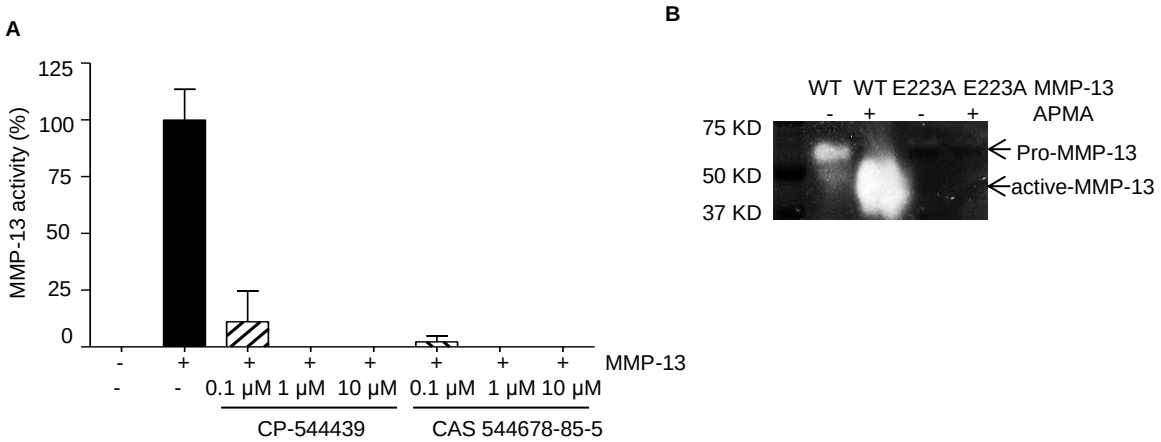

Supplemental Figure 7. Characterization of MMP-13 enzymatic activity. (A) Mouse non-adherent bone marrow cells were cultured with 200 ng/ml pro-MMP-13, and inhibitors CP544439 (0.1 μM, 1 μM or 10 μM), CAS 544678-85-5 (0.1 μM, 1 μM or 10 μM) or DMSO as control during OCL formation. The culture media were collected after 4 h and MMP-13 proteolytic activities were detected by MMP-13 fluorimetric assay (mean ± SD; n=3). The data are representative of 2 independent experiments. **(B)** 0.4 μg pro-MMP-13 WT or E223A protein were incubated with or without APMA (1 mM) in MMP-13 reaction buffer at 37°C for 20 minutes, then loaded into 10% SDS-PAGE gels containing 0.5% Collagen Type I. The gel was stained with Coomassie Brilliant Blue R250 and then de-stained. The data are representative of 2 independent experiments.

Supplemental Figure 8

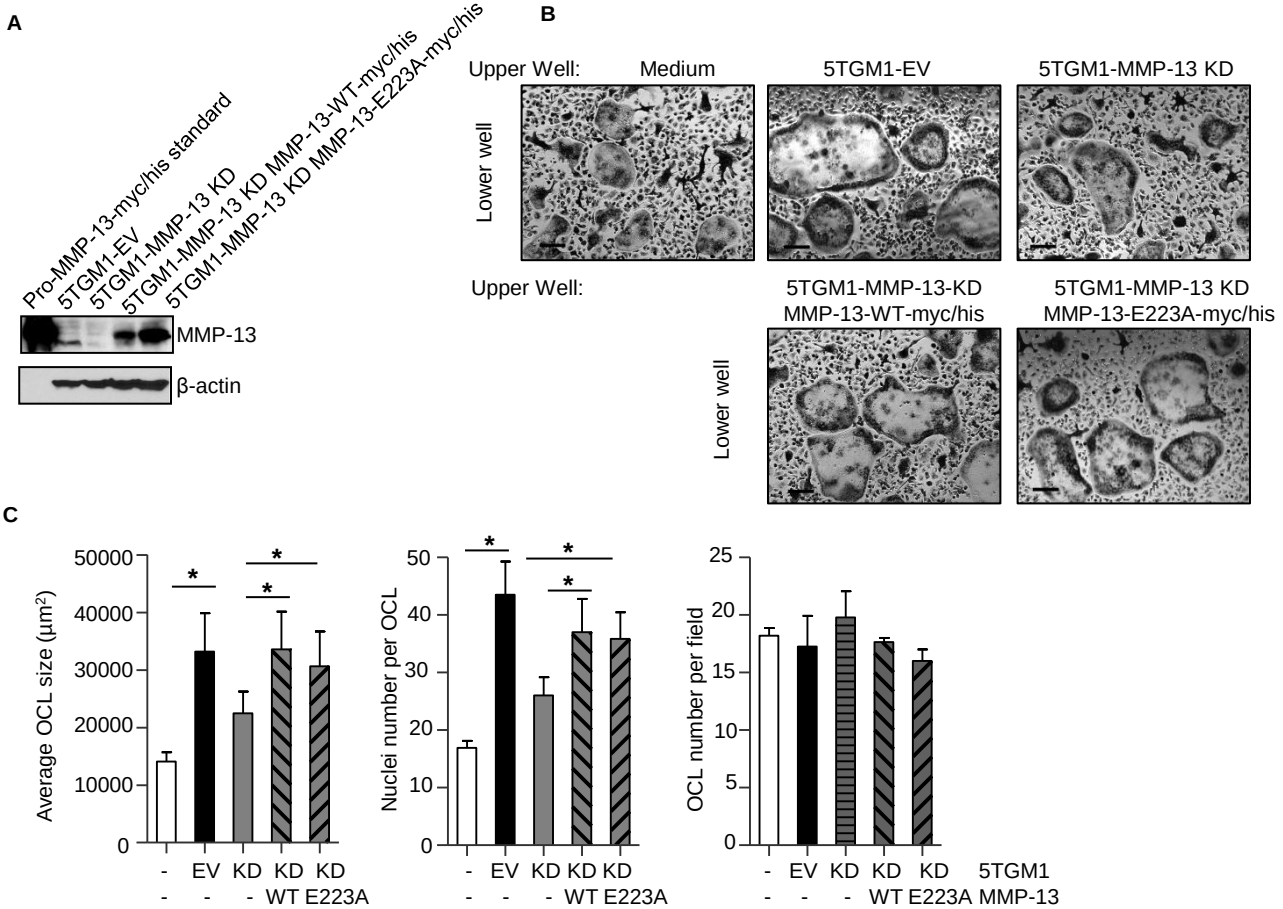

Supplemental Figure 8. MMP-13 E223A rescue 5TGM1 MMP-13 KD cells OCL induction effects. (A) 5TGM1 MMP-13 KD cells were infected by retrovirus expressing MMP-13-WT-myc/his or MMP-13-E223A-myc/his recombinant proteins and the stably infected cells were selected by hygromycin B selection. MMP-13 levels were detected in the whole cell lysates by WB. Purified Pro-MMP-13-WT-myc/his recombinant protein was loaded as positive control (Lane 1); β-actin was blotted as loading control. **(B-C)** Mouse non-adherent bone marrow cells were co-cultured with or without 5TGM1 cells in Transwell dishes in the presence of M-CSF (10 ng/ml) and RANKL (50 ng/ml) for 4 d to induce OCL differentiation. **(B)** OCLs were stained for TRAP and images captured as described in *Methods*. Scale bar, 100 μm. (**C)** OCL size (left panel), nuclei number per OCL (middle panel) and OCL number per field (right panel) were determined microscopically with ImageJ software (mean ± SEM; n=3). **P* ≤ 0.05, ***P* ≤ 0.01 by ANOVA (left panel) or Poisson ANOVA (middle and right panels). The data are representative of 2 independent experiments.

Supplemental Figure 9

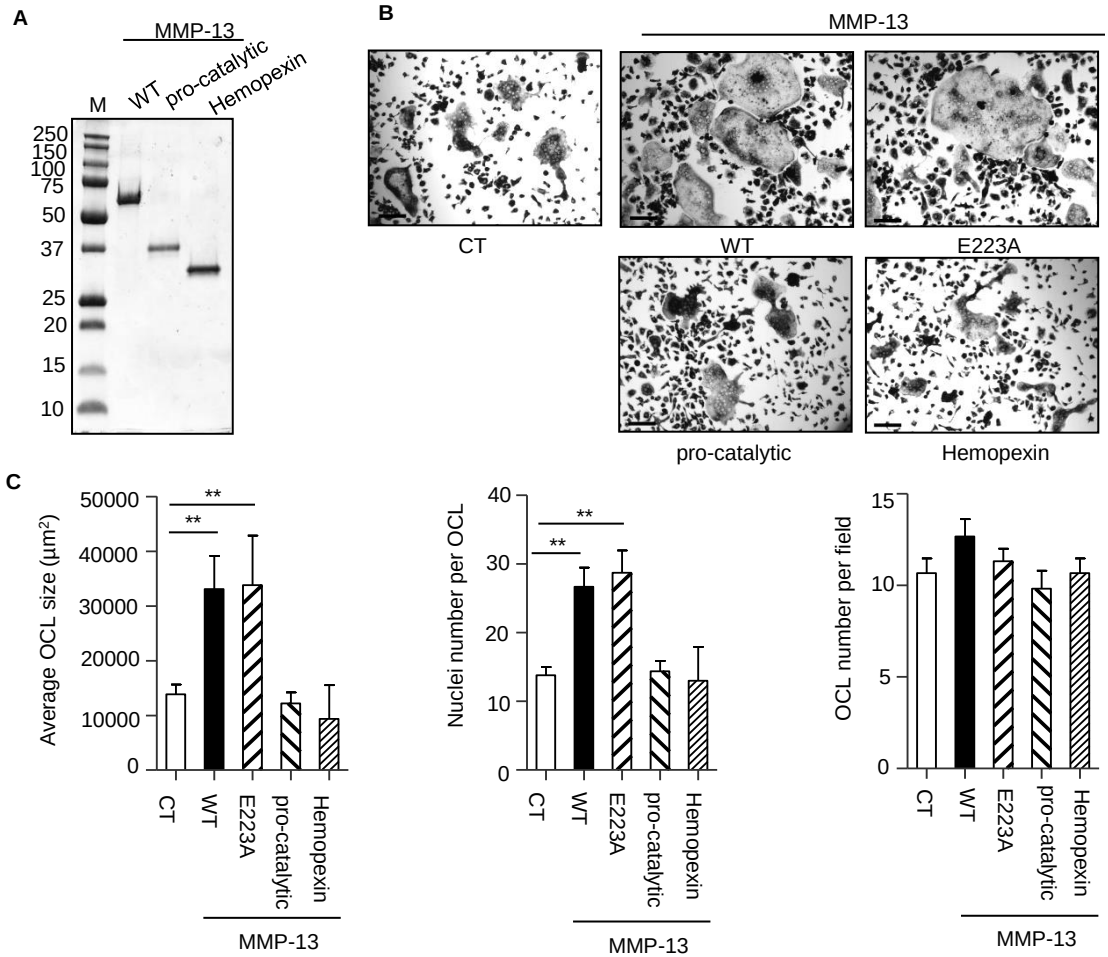

Supplemental Figure 9. MMP-13 catalytic or hemopexin domains fail to promote OCL fusion. (A) SDS/PAGE analysis of purified MMP-13 pro-catalytic domain (aa 1-267) and hemopexin domain (deletion aa 37-267). **(B)** Mouse non-adherent bone marrow cells were cultured with 200 ng/ml pro-MMP-13 WT, pro-MMP-13 E223A, the MMP-13 pro-catalytic domain, the MMP-13 hemopexin domain or vehicle (CT) during OCL formation in the presence of M-CSF (10 ng/ml) and RANKL (50 ng/ml). OCLs were stained for TRAP and images captured as described in *Methods*. Scale bar, 100 µm. The data are representative of 3 independent experiments. **(C)** OCL size (left panel), nuclei number per OCL (middle panel) and OCL number per field (right panel) were determined microscopically with ImageJ software (mean ± SEM; n=3). ***P* ≤ 0.01 by ANOVA (left panel) or Poisson ANOVA (middle and right panels).

Supplemental Figure 10

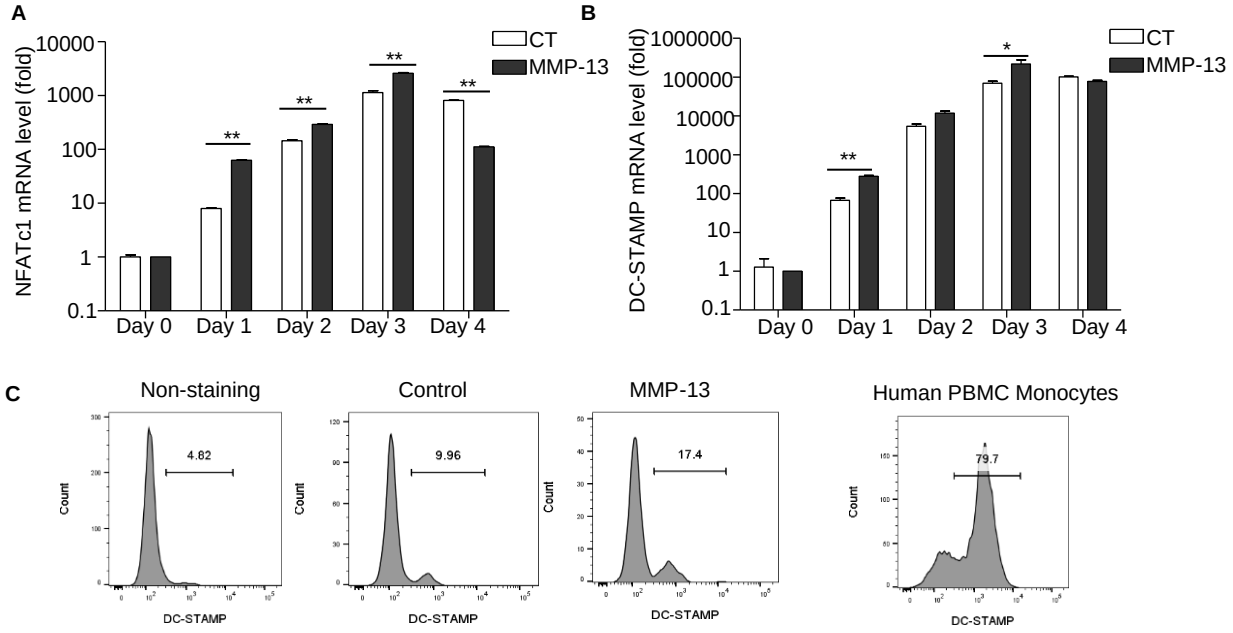

Supplemental Figure 10. MMP-13 upregulates NFATc1 and DC-STAMP mRNA expression and cell surface DC-STAMP. $CD11b^+$ cells from WT mice were selected from non-adherent bone marrow cells and cultured with RANKL (50 ng/ml) and M-CSF (10ng/ml) to induce osteoclastogenesis. MMP-13 (200 ng/ml) was added in the culture as indicated. **(A-B)** Cells were collected at the indicated time and NFATc1 (A) and DC-STAMP (B) mRNA levels were detected by Taqman real-time PCR (mean ± SD; n=3). β-actin was used as the internal control. $*P \leq 0.05$, $**P \leq 0.01$ by repeated measures ANOVA. The data are representative of 3 independent experiments. **(C)** Cells were collected at day 4 and cell surface DC-STAMP levels were detected by flow-cytometry assay (n=3). Human PBMC monocytes were stained as DC-STAMP positive control (right panel).

Supplemental Figure 11

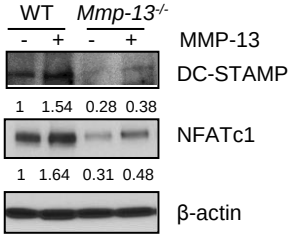

Supplemental Figure 11. *Mmp-13*$^{-/-}$ OCL display lower NFATc1 and DC-STAMP levels. CD11b^{+} cells from WT or *Mmp-13*$^{-/-}$ mice were selected from non-adherent bone marrow cells and cultured with RANKL (50 ng/ml) and M-CSF (10 ng/ml) for 5 d to induce osteoclastogenesis. MMP-13 (200 ng/ml) was added as indicated. Cell lysates were collected and subjected to Western blotting for DC-STAMP and NFATc1. β-actin was blotted as loading control. Band intensities were quantified by ImageJ, normalized to actin and compared to control. The relative intensities are shown. The data are representative of 3 independent experiments.

Supplemental Figure 12

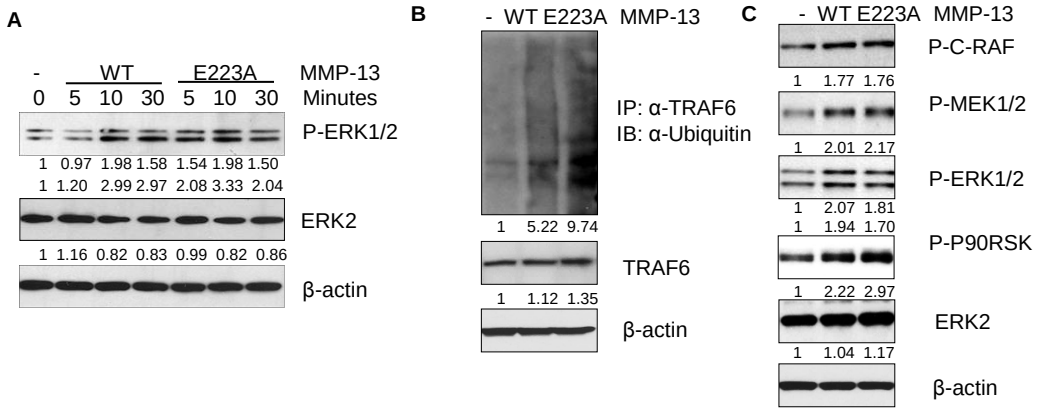

Supplemental Figure 12. MMP-13 triggers ERK1/2 phosphorylation independently of its catalytic activity. (A) Mouse CD11b$^+$ cells were selected from non-adherent bone marrow cells and cultured with RANKL (50 ng/ml) and M-CSF (10 ng/ml) for 3 d to induce osteoclastogenesis. Cells were treated with or without pro-MMP-13 WT or the pro-MMP-13 E223A mutant (200 ng/ml) for indicated times after serum starvation for 4 h. P-ERK1/2, ERK2 and β-actin levels were assessed by Western blotting. Band intensities were quantified by ImageJ, normalized to β-actin and compared to control. The relative intensities are shown. The data are representative of 2 independent experiments. **(B)** Mouse CD11b$^+$ cells were selected from non-adherent bone marrow cells and treated by RANKL (50 ng/ml) without or with pro-MMP-13 WT or the pro-MMP-13 E223A mutant (200 ng/ml) for 15 minutes. Cells were then lysed in RIPA buffer supplemented with 1% SDS and boiled for 10 minutes to denature proteins. Whole cell lysates were then diluted by 10X volume of RIPA buffer and incubated with 1 μg anti-TRAF6 antibody at 4C overnight. 20μl protein A/G agarose were was then added and incubated for 1 hour to pull-down the TRAF6 protein. TRAF6 ubiquitination was detected by anti-Ubi antibody after SDS-PAGE analysis. Band intensities were quantified by ImageJ, normalized to actin and compared to control. The relative intensities are shown. **(C)** Mouse CD11b$^+$ cells were selected from non-adherent bone marrow cells and treated by RANKL (50 ng/ml) without or with pro-MMP-13 WT or the pro-MMP-13 E223A mutant (200 ng/ml) for 10 minutes. Whole cell lysates were collected and subjected to WB to detect the activation of ERK signaling molecules with the indicated antibodies. Band intensities were quantified by ImageJ, normalized to actin and compared to control. The relative intensities are shown.

Supplemental Figure 13

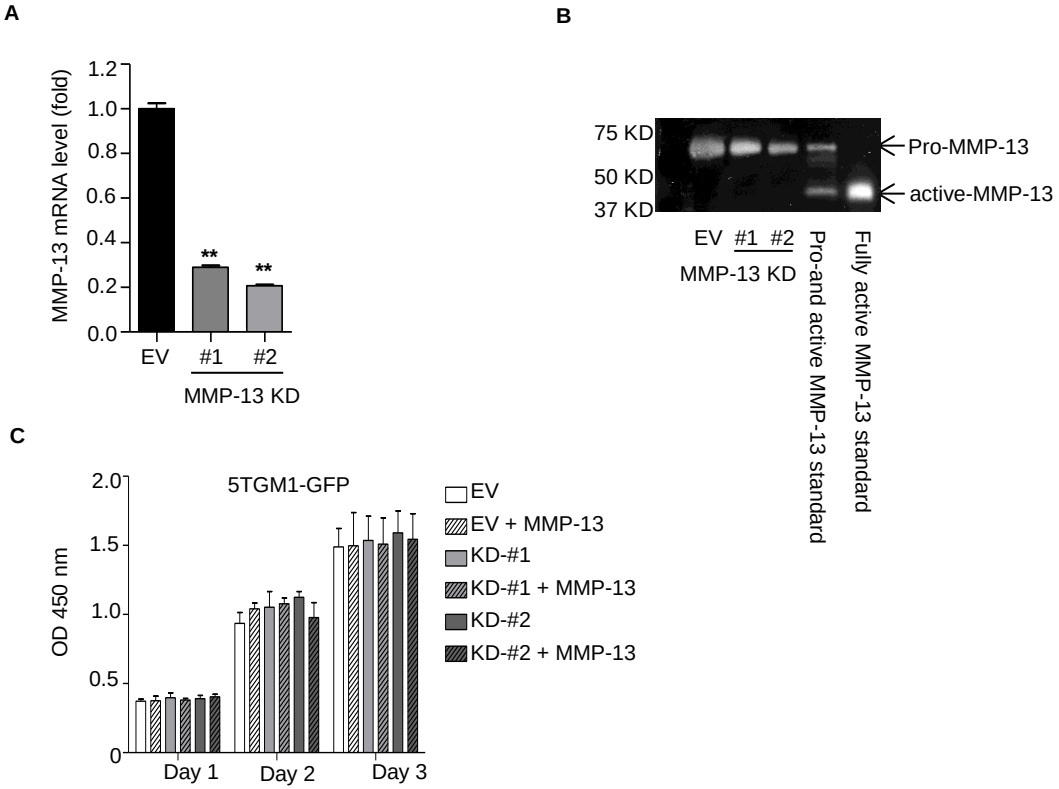

Supplemental Figure 13. Knockdown of MMP-13 in 5TGM1-GFP MM cells with MMP-13 targeting shRNA lentivirus. (A) MMP-13 mRNA expression levels were determined in 5TGM1-GFP-EV, 5TGM1-GFP-MMP-13 KD-#1 and KD-#2 cells by quantitative RT-PCR (mean ± SD; n=3). $^{**}P \leq 0.01$ by ANOVA. The data are representative of 3 independent experiments. **(B)** Supernatants from 5TGM1-GFP-EV, 5TGM1-GFP-MMP-13 KD-#1 and KD-#2 cells were concentrated and MMP-13 expression/processing determined by collagen zymography. A mixture of pro-MMP-13 (MW: 60 KD) and active MMP-13 (MW: 48 KD) or fully active MMP-13 protein (MW: 48 KD) standards were loaded as controls. The data are representative of 3 independent experiments. **(C)** 1×10^4 5TGM1-GFP-EV, 5TGM1-GFP-MMP-13 KD-#1 and KD-#2 cells were cultured with or without MMP-13 (200 ng/ml) for up to 3 d. Cell proliferation was determined by WST-1 assay. The data are representative of 3 independent experiments.

Supplemental Figure 14

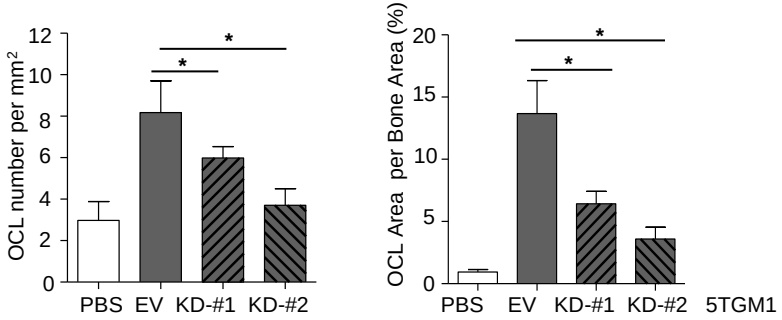

Supplemental Figure 14. MMP-13 KD in 5TGM1 MM cells decreased OCL size and number in vivo. OCL number per mm^2 and OCL surface per bone surface area from Figure 5 were determined microscopically with ImageJ software (mean ± SEM; n=6). *P ≤ 0.05 by ANOVA.

Supplemental Figure 15

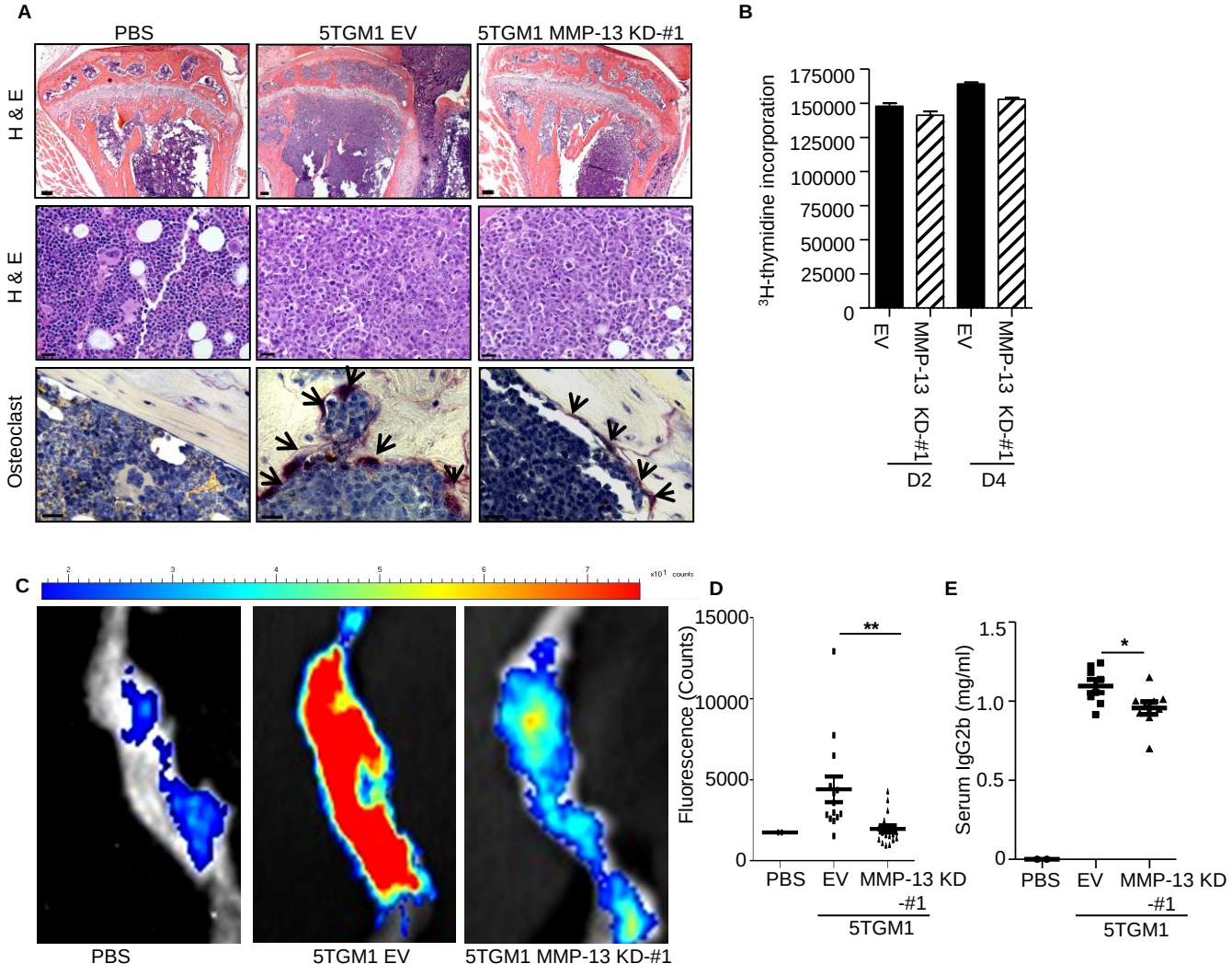

Supplemental Figure 15. MMP-13 KD impairs tumor progression *in vivo*. (A) PBS, 5TGM1-GFP-EV cells or 5TGM1-GFP-MMP-13 KD-#1 cells were injected bilaterally into both tibiae (n=18) *of Rag2*$^{-/-}$ mice. Mice were sacrificed 4 weeks later and the tibiae formalin-fixed followed by paraffin sectioning. Sections were then subjected to H&E and TRAP staining. Representative images are shown for each set of conditions. Scale bar, 100 μm. **(B)** 5TGM1-GFP EV or 5TGM1-GFP-MMP-13 KD-#1 cells were cultured in 200 μl culture medium for indicated times and DNA synthesis determined by ^{3}H-thymidine incorporation (mean ± SD; n=6). **(C-D)** Mice tibiae from (A) were imaged for GFP fluorescence intensity (C) before formalin fixation and fluorescence counts quantified (mean ± SD; n=18) (D), reflecting MM tumor burden. $^{**}P \leq 0.01$ by Student's *t*-test. Representative images are shown for each condition (C). **(E)** Mouse serum IgG2b levels were quantified by ELISA assay at the 4 week termination endpoint (mean ± SEM; n=9). $^{*}P \leq 0.05$ by Student's *t*-test.

Supplemental Figure 16

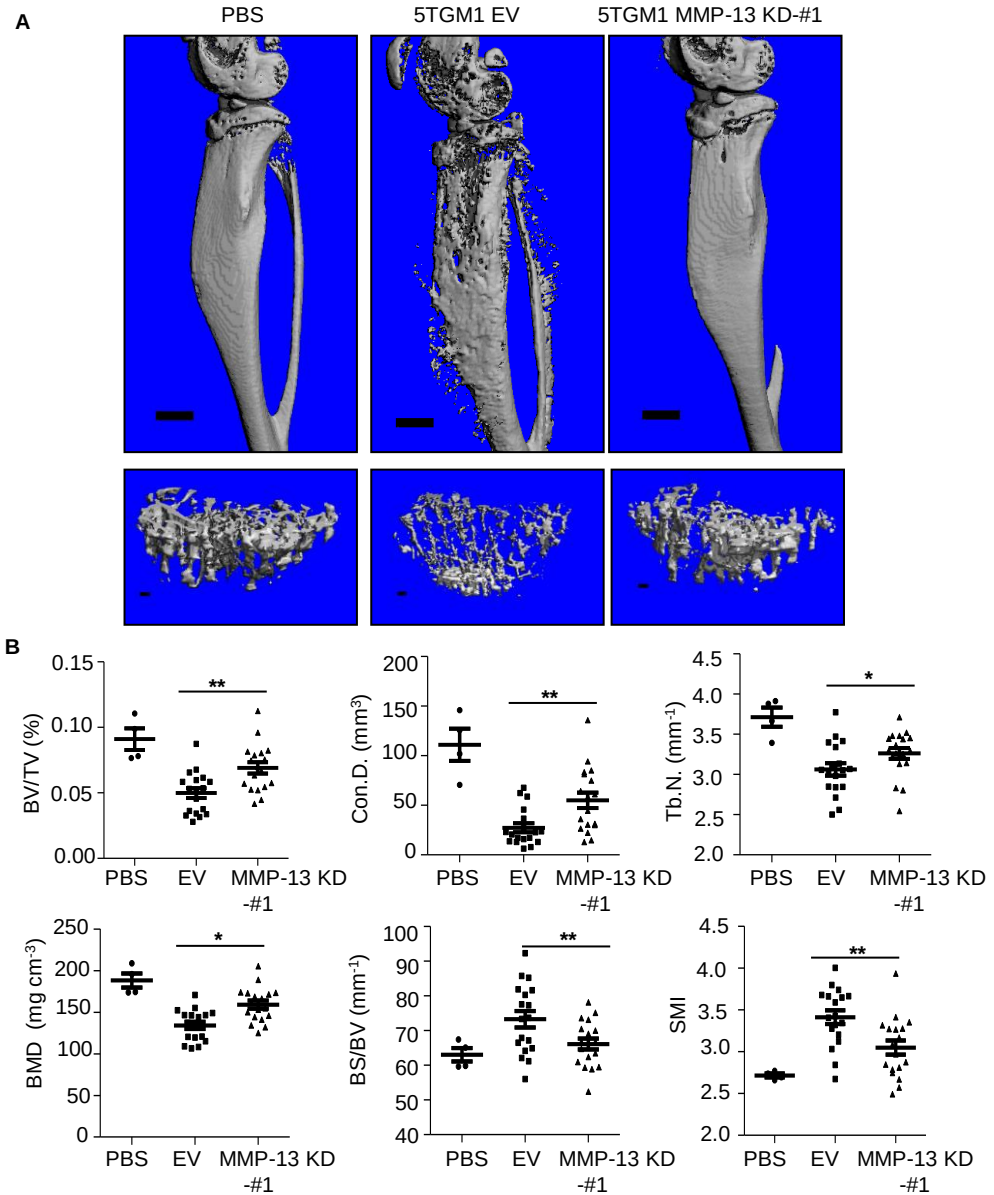

Supplemental Figure 16. MMP-13 directs MM-induced osteolysis. (A) PBS, 5TGM1-GFP-EV cells or 5TGM1-GFP-MMP-13 KD-#1 cells were injected bilaterally into both tibiae (n=18) of *Rag2*$^{-/-}$ mice. Mice were sacrificed 4 weeks later and the tibiae were formalin-fixed followed by 3D micro-CT scanning. Representative 3D images of tibiae, adjacent femurs (upper panel) and tibiae trabecular bones (lower panel) from each treatment regimen are shown. Upper panel scale bar, 1 mm. Lower panel scale bar, 100 μm. **(B)** Trabecular bone of mice tibiae from (A) were analyzed and micro-structural parameters, including bone volume fraction (BV/TV), connective density (Con.D.), trabecular number (Tb.N.), bone mineral density (BMD), bone surface to volume ratio (BS/BV) and structure model index (SMI) determined (mean ± SEM; n=18). **P* ≤ 0.05, ***P* ≤ 0.01 by Student's *t*-test.

Supplemental Figure 17

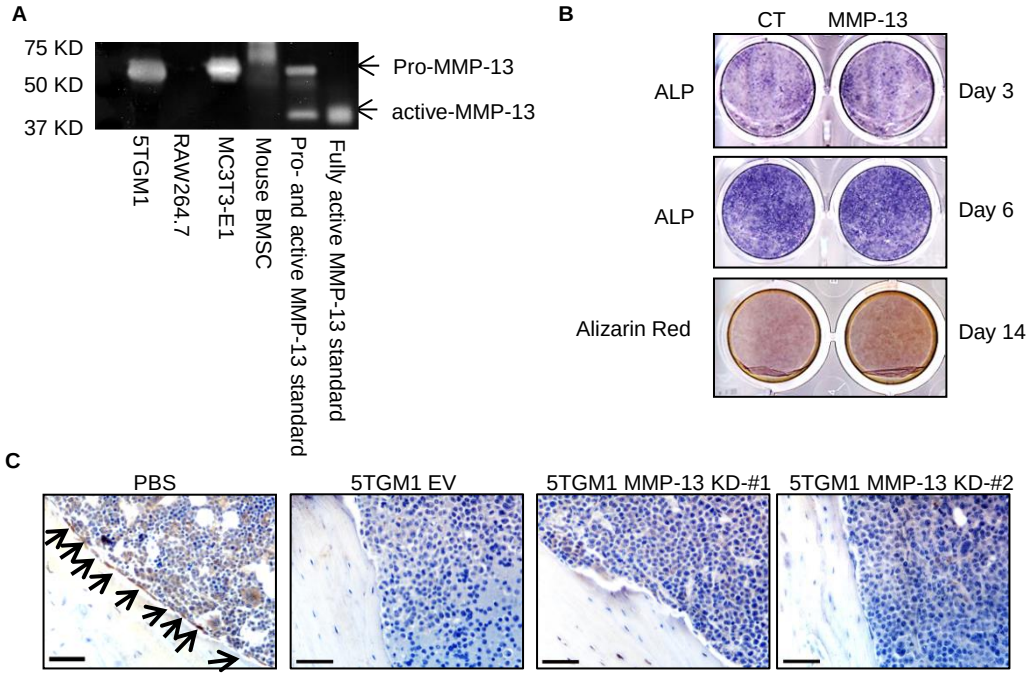

Supplemental Figure 17. MMP-13 expression and osteoblastogenic activity. (A) Supernatants from human MM cell line RPMI-8266, mouse MM cells line 5TGM1, mouse pre-osteoclast cell line RAW 264.7, mouse pre-osteoblast cell line MC3T3-E1, or primary mouse bone marrow stromal cells (BMSC) were concentrated and MMP-13 expression/processing determined by collagen zymography. A mixture of pro-MMP-13 (MW: 60 KD) and active MMP-13 (MW: 48 KD) or fully active MMP-13 protein (MW: 48 KD) standards were loaded as controls. **(B)** $1x10^4$ MC3T3-E1 cells were cultured in osteoblast differentiation media with or without MMP-13 (200 ng/ml) for up to 14 d. Osteoblast cells were fixed and followed by ALP staining or alizarin red staining as indicated (n=3). **(C)** PBS, 5TGM1-GFP-EV cells or 5TGM1-GFP-MMP-13 KD cells control were injected bilaterally into the tibiae (n=18) of *Rag2*$^{-/-}$ mice. Mice were sacrificed 4 weeks later and the tibiae formalin-fixed followed by paraffin sectioning. Sections were then subjected to IHC staining by osteocalcin antibody for osteoblast cells. Representative images are shown for each set of conditions. Scale bar, 100 μm.

Supplemental Figure 18

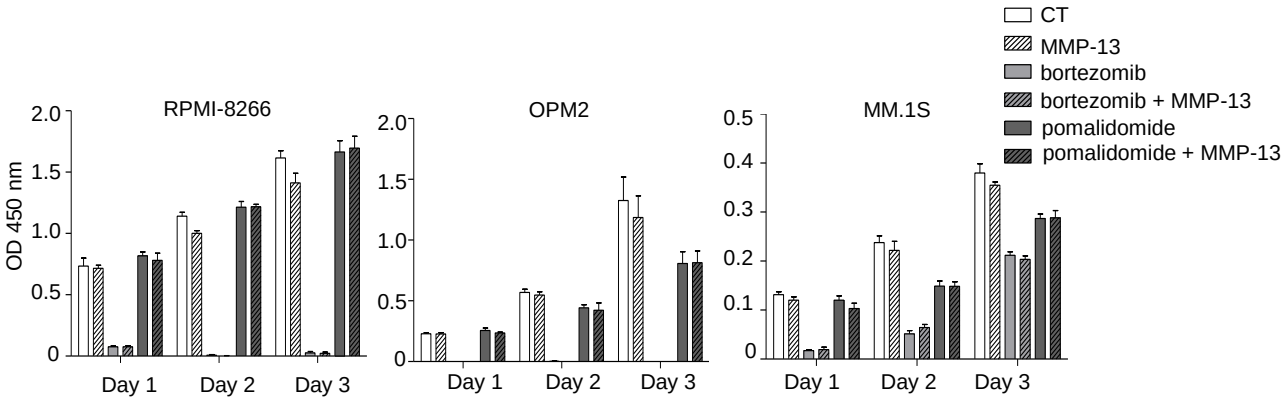

Supplemental Figure 18. MMP-13 has no effects on MM cell proliferation or anti-MM agents sensitivity. 1×10^4 MM cells were treated with anti-MM agents, bortezomib (100 nM), or pomalidomide (2 μM) with or without MMP-13 (200 ng/ml) for up to 3 d. DMSO was added in control groups (CT). Proliferation was determined by WST-1 assay. The data are representative of 3 independent experiments.